

**COMBINED TEM AND NANOSIMS ANALYSIS OF SUBGRAINS IN A SiC AB GRAIN.** K. M. Hynes<sup>1</sup>, S. Amari<sup>1</sup>, T. J. Bernatowicz<sup>1</sup>, E. Lebsack<sup>1</sup>, F. Gyngard<sup>2</sup>, and L. R. Nittler<sup>2</sup>, <sup>1</sup>Laboratory for Space Sciences and Department of Physics, Washington University, St. Louis, MO 63130, [khynes@physics.wustl.edu](mailto:khynes@physics.wustl.edu), <sup>2</sup>Department of Terrestrial Magnetism, Carnegie Institution of Washington, Washington, DC 20015.

**Introduction:** SiC AB grains, which comprise ~4 – 5% of the total presolar SiC population, are defined as having  $^{12}\text{C}/^{13}\text{C} < 10$  [1]. These grains have a wide range of  $^{14}\text{N}/^{15}\text{N}$  ratios ( $39 \leq ^{14}\text{N}/^{15}\text{N} \leq 9800$ ) and Si isotopes similar to mainstream SiC grains. Roughly half of AB grains contain *s*-process enrichments, while the rest have solar *s*-process elemental abundances. The isotopic signatures of AB grains cannot be easily explained by theoretical models of nucleosynthesis in asymptotic giant branch (AGB) stars [2]. Instead, J stars have been proposed as the most likely source of AB grains with no *s*-process enrichments, while born-again AGB stars may be the parent stars of AB grains with *s*-process enrichments and high  $^{14}\text{N}/^{15}\text{N}$  ratios [1].

Structural and chemical microanalysis of presolar grains with the transmission electron microscope (TEM) can provide valuable information on the conditions under which these grains condensed, as well as reveal the possible presence of internal subgrains. When combined with isotopic analysis, the most complete picture of grain formation emerges. However, only a handful of AB grains have been analyzed for their isotopic, chemical, and structural properties, as well as for the presence of subgrains [3, 4]. Here we present data from the coordinated microanalysis of one AB grain and its unusual subgrains.

**Experimental:** AB grains from the KJG size fraction of the Murchison meteorite (~3  $\mu\text{m}$  average diameter [5]) were first identified by their low  $^{12}\text{C}/^{13}\text{C}$  ratios by ion imaging in the IMS-3f ion probe [1]. The C, Si, and N isotopic compositions of these grains were then measured in the Washington University NanoSIMS. Seven randomly selected AB grains were prepared for TEM study and sliced into 70-nm-thick slices with a diamond ultramicrotome. The grains were subsequently analyzed in a JEOL 2000FX TEM equipped with an Energy Dispersive X-ray Spectrometer (EDXS). After TEM analysis, AB grain KJG-N4-468-1 was selected for additional analysis on the basis of its unusual subgrains. One TEM grid containing several slices of this AB grain was re-mounted for isotopic analysis. Finally, negative secondary ion images of  $^{28}\text{Si}$ ,  $^{32,33,34,36}\text{S}$ ,  $^{40}\text{Ca}$ ,  $^{16}\text{O}$ , and  $^{56}\text{Fe}$ ,  $^{16}\text{O}$  were simultaneously acquired with the Carnegie NanoSIMS 50L for each slice of KJG-N4-468-1.

**Results and Discussion:** The C, N, and Si isotopic compositions of grain KJG-N4-468-1 are typical of an AB grain, with  $^{12}\text{C}/^{13}\text{C} = 2.75 \pm 0.01$ ,  $^{14}\text{N}/^{15}\text{N} = 351.6 \pm 6.1$ ,  $\delta^{29}\text{Si}/^{28}\text{Si} = -0.36 \pm 2.40$ , and  $\delta^{30}\text{Si}/^{28}\text{Si} = -4.47 \pm$

3.36. TEM microdiffraction patterns revealed that the grain is composed of at least seven crystal domains, with observed diameters ranging from 135 – 746 nm. These domains were all indexed to either the 3C polytype (fcc;  $a = 4.35 \text{ \AA}$ ), the 2H polytype (hexagonal;  $a = 3.08 \text{ \AA}$ ,  $c = 5.03 \text{ \AA}$ ), or an intergrowth of the two. These polytypes are consistent with those previously observed in presolar SiC [6].

EDXS analysis indicated solar abundances of *s*-process elements in KJG-N4-468-1, suggesting that a J star origin is most likely for this SiC grain. Sixteen subgrains, ranging from 17 – 41 nm in diameter, were also discovered during EDXS analysis of KJG-N4-468-1. Three of the subgrains were identified as TiC (fcc;  $a = 4.39 \text{ \AA}$ ). These subgrains are euhedral, with microdiffraction patterns clearly indicating an epitaxial alignment with the surrounding SiC. Seven subgrains were conclusively identified as oldhamite (CaS; fcc;  $a = 5.696 \text{ \AA}$ ). Although it has been predicted as a stable circumstellar condensate [7, 8], this is the first observation of oldhamite in presolar grains. Crystallographic analysis revealed that all of the oldhamite subgrains are anhedral (Figure 1), with no evidence of the crystal faces remaining, and also showed that the oldhamite is epitaxially aligned with the surrounding SiC. The final five subgrains observed in KJG-N4-468-1 are Fe-rich. Due to the location of the SiC slices on the sample mount, a conclusive determination of the mineralogy of these grains was not possible. However, diffraction patterns obtained from the Fe-rich subgrains, combined with EDXS analysis, suggests that the subgrains are most likely Fe carbide. These subgrains are euhedral and epitaxially aligned with the surrounding SiC. Grain KJG-N4-468-1 was the only grain of the seven AB grains in this study to contain oldhamite or Fe-rich subgrains [3, 4].

All five Fe-rich subgrains in KJG-N4-468-1 were in close proximity (9 – 38 nm) to an oldhamite subgrain (Figure 1). This strongly suggests that a relationship between the two types of subgrains exists, but the specific nature of this relationship is not clear. The anhedral morphology of the oldhamite seems indicative of back-reaction or phase instability, but it is also unclear if this is a result of a formational relationship between the oldhamite and the Fe-rich subgrains or if it is independent of the proximity of the subgrains.

The location of all of the subgrains along the SiC crystal domain boundaries, coupled with the epitaxial alignment between the subgrains and the SiC, strongly

suggests that the subgrains condensed in solid-solution with the SiC and later exsolved. This formation mechanism for TiC, which is isostructural with SiC, is consistent with previous observations of TiC subgrains in presolar SiC [e.g., 9, 10], as well as with theoretical predictions [11]. Oldhamite and Fe carbide, however, have significantly different structural properties from SiC and are therefore not predicted to form readily in solid solution with it [11], contrary to the observations of this study. Thermodynamic calculations predict TiC to condense in solid solution with SiC at 1544 K, followed by Fe carbide and oldhamite at 1252 K [8]. The presence of refractory TiC subgrains in the same SiC grain with comparatively low temperature oldhamite and Fe carbide subgrains suggests that thermochemical equilibrium must have been maintained over a large temperature range in the stellar environment where this SiC grain condensed.

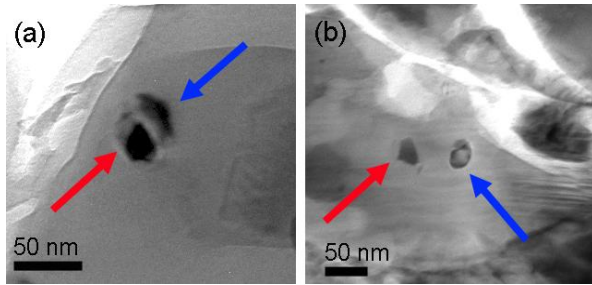


**Figure 1.** Bright-field (BF) TEM images showing two examples of oldhamite subgrains (blue arrows) and nearby Fe-rich subgrains (red arrows) located  $\sim 9$  nm apart (a) and  $\sim 34$  nm apart (b). All four subgrains are located in a single slice of KJG-N4-468-1.

Sulfur isotopic images were successfully obtained with the NanoSIMS for 5 slices of KJG-N4-468-1 (Figure 2). In at least 3 of the slices, hotspots of S were observed within the grain and were correlated with Ca and Fe, consistent with the TEM observations of oldhamite subgrains with Fe-rich subgrains located nearby. Due to their small size, the S isotopic composition was not able to be quantified for most of the subgrains; however, one subgrain may have an enrichment in  $^{34}\text{S}$  ( $\delta^{34}\text{S}/^{32}\text{S} = 70 \pm 37 \text{‰}$ ), along with normal  $^{33,36}\text{S}$ , within errors. This enrichment in  $^{34}\text{S}$  is likely a lower limit, as the limited spatial resolution of the primary beam can dilute the subgrain's true S composition with solar. Models for  $2 M_{\odot}$  AGB stars of close-to-solar metallicity predict only modest enrichments in  $^{34}\text{S}$  of  $\sim 11\text{‰}$  [12].

**Acknowledgements:** We thank Rhonda Stroud (Naval Research Laboratory) for her help preparing the TEM grid for NanoSIMS analysis and Roy Lewis

(University of Chicago) for providing the Murchison KJG samples.

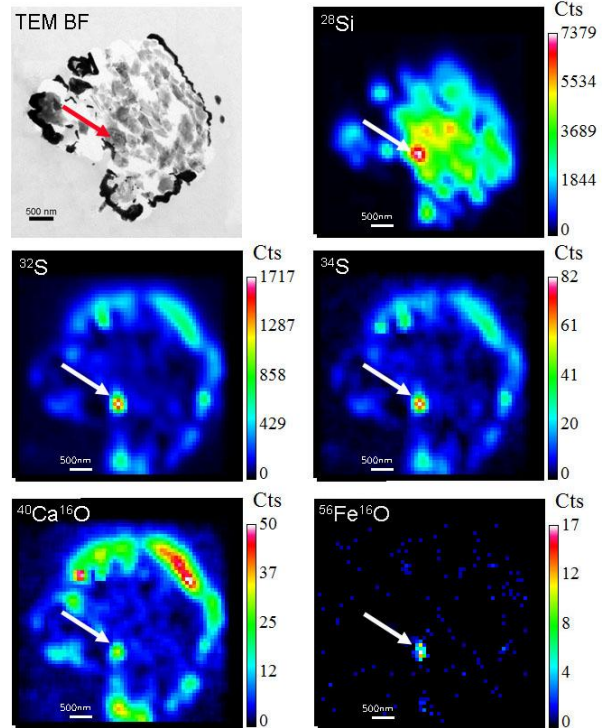


**Figure 2.** TEM BF image and corresponding NanoSIMS ion images of  $^{28}\text{Si}$ ,  $^{32}\text{S}$ ,  $^{34}\text{S}$ ,  $^{40}\text{Ca}^{16}\text{O}$ , and  $^{56}\text{Fe}^{16}\text{O}$  for one slice of KJG-N4-468-1. A S hotspot is indicated by an arrow in each of the images. The Ca and Fe signals are correlated with the S, which is strongly indicative of an oldhamite subgrain with a nearby Fe-rich subgrain, and is consistent with TEM observations.

**References:** [1] Amari S. et al. (2001) *ApJ*, 559, 463-483. [2] Meyer B. S. and Zinner E., in *MESS II*, Lauretta D. S., McSween H. Y., Jr., Eds. (Univ. of Arizona, Tucson, 2006) pp. 69-108. [3] Hynes K.M. et al. (2010) *LPS XLI*, Abstract #2074. [4] Hynes K.M. et al. (2010) *Meteoritics & Planet. Sci.*, 45, 596. [5] Amari S. et al. (1994) *Geochim. Cosmochim. Acta*, 58, 459-470. [6] Daulton T.L. et al. (2003) *Geochim. Cosmochim. Acta* 67, 4743-4767. [7] Sharp C. M. and Wasserburg G. J. (1995) *Geochim. Cosmochim. Acta* 59, 1633-1652. [8] Lodders K. and Fegley B., Jr. (1995) *Meteoritics* 30, 661-678. [9] Stroud R.M. and Bernatowicz T.J. (2005) *LPS XXXVI*, Abstract #2010. [10] Bernatowicz T.J. et al. (1992) *LPS XXIII*, 91. [11] Upadhyaya G.S., *Nature and properties of refractory carbides* (Nova Science Publishers, Commack, N.Y., 1996), 545 p. [12] Gallino R., personal communication.